J. Synchrotron Rad. (1998). **5**, 275–279

Avalanche Photodiodes as Fast X-ray Detectors

Shunji Kishimoto

Photon Factory, Institute of Materials Structure Science, 1-1 Oho, Tsukuba, Ibaraki 305, Japan. E-mail: kisimoto@kekvax.kek.jp

(*Received 4 August 1997; accepted 6 January 1998*)

An avalanche photodiode (APD) detector provides a sub-nanosecond time resolution and an output rate of more than 10^8 counts s^{-1} of synchrotron X-rays. Moreover, the APD has the advantage of low noise. A review of recent developments of detectors using APD devices designed for X-ray experiments is presented in this paper. One of the detectors has an excellent time response of 100 ps resolution and a narrow width on its response function, 1.4 ns at 10^{-5} maximum. The other consists of a stack of four diodes and has a transmission structure. The stacked detector improved the efficiency for X-rays, *e.g.* 55% at 16.53 keV. The output rates reached more than 10^8 counts s^{-1} per device.

Keywords: avalanche photodiodes; time resolution; fast counting.

1. Introduction

The time response of avalanche photodiodes (APDs) is in the sub-nanosecond range. In addition, APDs have an internal gain of 10^2–10^3. They are suitable for observing a fast pulse created by a single X-ray photon. The fast response of APDs was first used in Mössbauer time spectroscopy as an application in studies using synchrotron radiation. We used a detector with an S2384 device (Hamamatsu Photonics). The detector provided a sub-nanosecond time resolution of 0.26 ns (FWHM) in nuclear resonance measurements of ^{57}Fe (Kishimoto, 1992).

During the past five years, other APD devices have also been used for Mössbauer time spectroscopy using synchrotron radiation (Baron & Ruby, 1994; Toellner *et al.*, 1994; Baron, 1995). However, the existing silicon APDs have some limitations in detecting X-rays, such as tail profiles in time response, *e.g.* 10 ns long at 10^{-5} maximum for S2384, and a relatively small efficiency for X-rays. Some detectors have been developed using APD devices designed for experiments using synchrotron X-rays. This paper reviews applications with a 100 ps time resolution and introduces the development of a new detector for high counting rates.

2. Characteristics of avalanche photodiodes

For directly detecting X-rays, an avalanche photodiode can be considered as a solid-state detector. Silicon APDs are widely used and have structures of p-type and n-type layers, just like an Si(Li) detector. Two types are well known: the reach-through and the bevelled-edge (Webb *et al.*, 1974; Squillante *et al.*, 1986). As shown in Fig. 1, each type has a thin depletion layer of up to 100 μm. A high electric field of more than 2×10^4 V cm^{-1} is applied to the depletion region in the reach-through type, for example. The thin depletion layer and the high electric field are characteristic of the APD. When an X-ray arrives at the depletion region, photoelectrons caused by the photoelectric effect generate electron–hole pairs. The carriers are collected at each electrode in the high electric field of the drift region. The electron carriers are multiplied in a p–n (n^+) junction and the APD has an internal gain of 10^2–10^3. Thus, we can observe fast signals of the order of

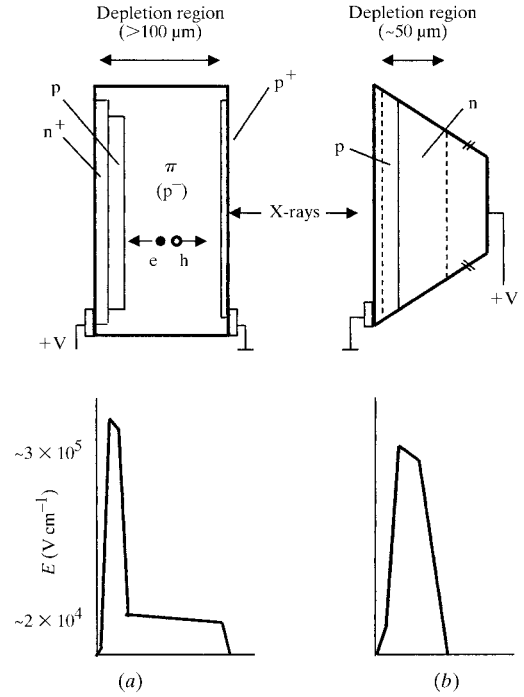

Figure 1
Structures of silicon avalanche photodiodes: (*a*) reach-through type and (*b*) bevelled-edge type.

nanoseconds for a single X-ray photon if we develop a detector with a fast amplifier having a gain of more than 100.

3. Applications of excellent time resolution

Applications of excellent time resolution were carried out with an APD detector using an S5343 device. The device was developed by Hamamatsu Photonics. Compared with other devices, it has a thinner depletion layer, of 9 μm. The thin depletion layer is fabricated by the epitaxic growth on the n^+ wafer. This is one of the reach-through devices in view of the field structure. The efficiency of the device was 12% at 8.05 keV (Kishimoto, 1994).

We measured the bunch purity of a storage ring with the detector at the Photon Factory ring (Kishimoto, 1994). A time resolution of 100 ps and a short tail of 1.4 ns at 10^{-5} maximum enabled us to observe a small sub-bunch, adjacent to the main bunch, corresponding to a purity of 6×10^{-9}. The 100 ps resolution is useful for observing the short-width bunch profile of the third-generation ring and experiments using this property. Fig. 2 shows a bunch profile in the hybrid mode of the ESRF ring, measured with another detector using S5343 at beamline ID18. The ESRF ring has a 2.8 ns bunch interval. The bunch width was calculated using an observed peak width (ΔT) of 115 ps and the detector resolution of 100 ps, which was already known by other measurements, according to the equation

$$\Delta T^2 = \Delta T_B^2 + \Delta T_D^2, \qquad (1)$$

where ΔT_B is the bunch width and ΔT_D is the time resolution of the detector system. The value of ΔT_B was given as 60 ps. This was consistent with the value of 62 ps measured by a streak camera (Sheidt, 1995).

4. Detector using a stack of four APDs (SPL2625)

A new detector using a stack of APDs has been developed at the Photon Factory. This detector was developed for

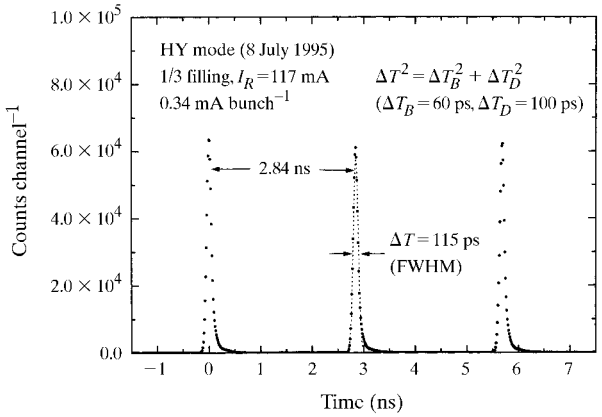

Figure 2
Bunch profile observed in the hybrid mode of the ESRF. This spectrum was measured on 8 July 1995.

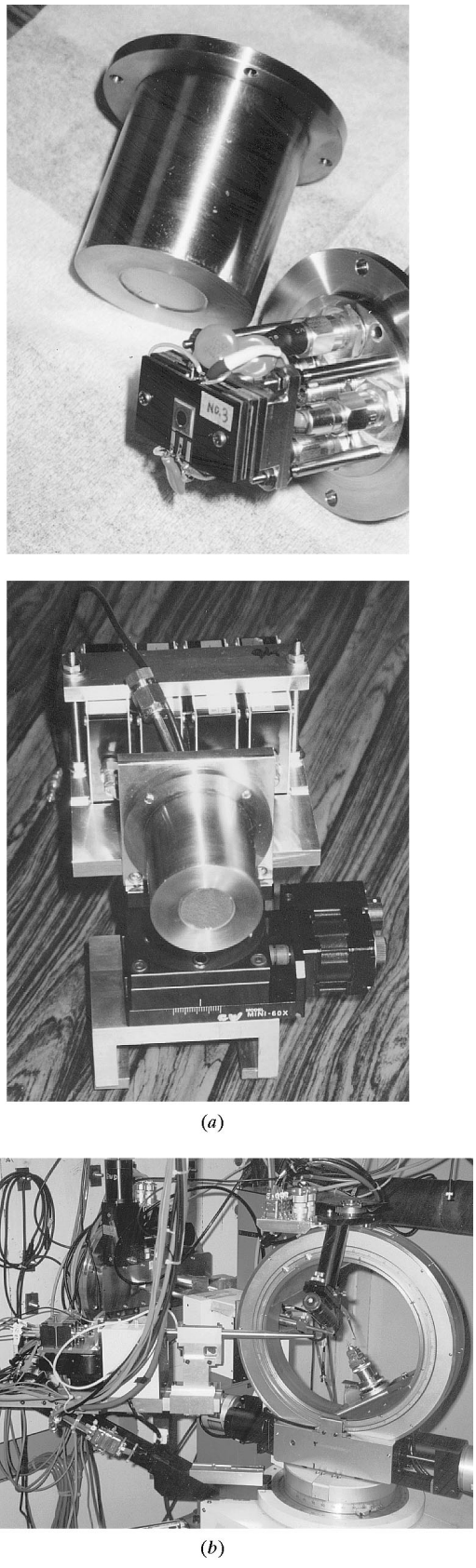

(*a*)

(*b*)

Figure 3
Photographs of the APD detector using a stack of four SPL2625s: (*a*) the stack of four devices (top) and the out view of the detector (bottom), (*b*) the detector installed at a four-circle diffractometer of BL14A at the Photon Factory.

applications with high counting rates, such as X-ray diffraction experiments in electron density studies (Kishimoto *et al.*, 1998). New SPL2625 devices (Hamamatsu Photonics) are used for the detector. This device is a prototype of transmission structure. This means that the device has thin dead regions on the surfaces of the device and no metallic layers inside the sensitive area. A thick sensitive region of more than 120 μm was designed to obtain a large efficiency for high-energy photons. The detector system and the counting properties are explained here and the details are described by Kishimoto *et al.* (1998).

By stacking the APDs we can obtain a larger efficiency compared with using a single device. A thickness of 480 μm silicon was obtained by stacking and the efficiency was 55% at 16.53 keV. This value is three times as large as that of a single device (18%). Fig. 3(*a*) shows the stack of four APDs. The sensitive area is 2.8 mm in diameter. The chamber size is 40 mm in diameter. Each device is connected to a fast amplifier (Phillips Scientific 6954). Fig. 3(*b*) shows that the detector is installed on the 2θ arm of a four-circle diffractometer installed at beamline BL14A of the Photon Factory. Fig. 4 shows a simple system for fast counting. The detector has four independent channels of the APD device. Output pulses from each amplifier are processed by a discriminator (Technoland Co. C-TM415). The width of the output pulse was shorter than 4 ns on the base line. The rise time was about 1 ns. The output pulse of the discriminator also had a width shorter than 4 ns on the baseline. If a pulse splitter is used before the discriminator, the number of counts in a window width is obtained by subtraction of the counts between the lower level and the upper level of the discriminator. The setting of a threshold level of the discriminator and the recording of the counts of the 300 MHz scaler (Technoland Co. C-KP402) were controlled by a personal computer through CAMAC.

The behaviour of the output rate was investigated using direct beams of synchrotron X-rays from the Photon Factory ring. The X-ray energy was 16.53 keV. The result is shown in Fig. 5. The solid circles show the sum of output rates of the four channels. The open circles show the output rate of the front device (channel 1). The input rate was obtained with an NaI(Tl) scintillation detector and attenuators of molybdenum foils. The solid and dashed curves correspond to the paralyzable model and the non-paralyzable model for pulsed X-rays, respectively. Fig. 6 schematically shows a model of the counting system for the pulsed beams, considering the pulsed nature of synchrotron radiation (Kishimoto, 1997). According to the model, the behaviours are given by (*a*) for the paralyzable model,

$$m = \sum_{i=1}^{4} f'[1 - \exp(-\varepsilon_i n/f')] \exp[-(k-1)\varepsilon_i n/f'], \quad (2)$$

and (*b*) for the non-paralyzable model,

$$m = \sum_{i=1}^{4} \frac{f'[1 - \exp(-\varepsilon_i n/f')]}{1 + (k-1)[1 - \exp(-\varepsilon_i n/f')]}. \quad (3)$$

Here, m is the output rate and n is the input photon rate. The symbol f' indicates the number of bunches observed in unit time. This is given by the bunch frequency f (500.1 MHz) and the bunch structure for the multibunch mode of the Photon Factory ring (Fig. 6*c*), as $f \times 280/312$. The efficiency of each APD channel (i = 1–4) is expressed by ε_i. k is an integer determined by the relation $T + (k-1)/f < \tau < k/f$. Here, T is the bunch width and τ is the dead time of the system. τ is shorter than 4 ns, considering the observed pulse width. Thus, $k = 2$ is applied to the model equations for the present system. Equation (2) gives a better fit to the result at input photon rates lower than 1.5×10^9 photons s^{-1}. At higher rates the model does not explain the observed behaviour. The discriminator might not have an ideal response because the input signals overlap each other and their shape is

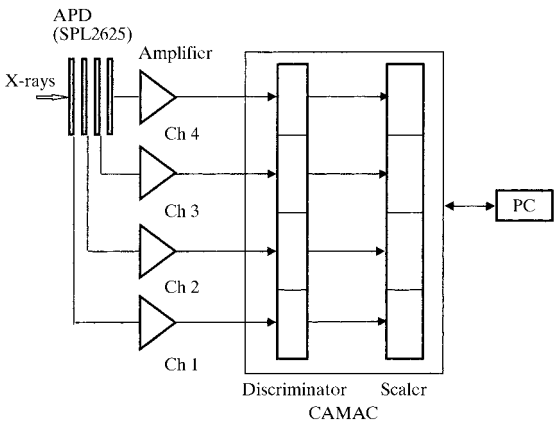

Figure 4
A simple fast-counting system with the detector using stacked APD devices. (Ch = channel.)

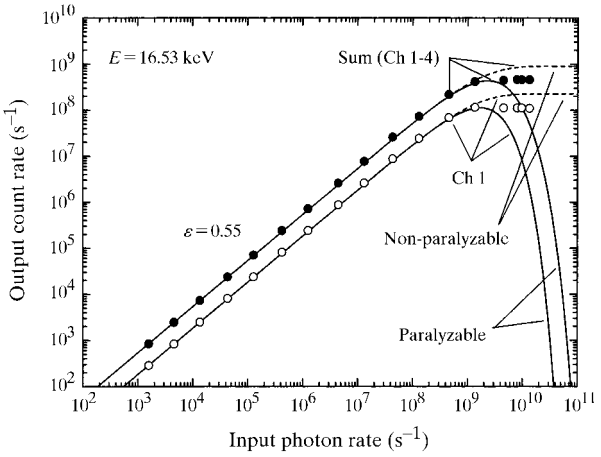

Figure 5
Behaviour of the output rate as a function of the input photon rate, measured at 16.53 keV. Closed circles show the output rates for the sum of four channels and open circles are for the output rates of the front device (channel 1). Solid curves are plotted using equation (2) and dashed curves are given by equation (3).

greatly changed from that of a single pulse. However, the count rate reached 4.5×10^8 counts s^{-1} as the sum of the four channels. Since the noise level was 10^{-2} counts s^{-1}, the dynamic range of the output rate is more than 10^{10}.

The time response of this device is shown in Fig. 7(*a*). The vertical axis is given by a logarithmic scale. The FWHM time resolution is 1.2 ns for 14.4 keV X-rays. At 10^{-5} maximum, the width is 2.75 ns, and does not broaden much. If the time resolution of 1.2 ns is accepted, we can use this device for experiments in time spectroscopy. On the other hand, Fig. 7(*b*) shows the response function, in which the vertical axis is given by a linear scale. The X-ray beam was irradiated from the p–n^+ junction side of the APD device in this experiment. Energies of 8.0, 10.0, 14.4 and 17.7 keV were used for observing the energy dependence of the response function. The curves observed at these energies are plotted in Fig. 7(*b*) after normalization of the peak height to the result at 14.4 keV. These curves are almost explained by the distribution of X-ray absorption through the drift region of about 100 μm and by the peak of signals generated in the multiplication region. The dashed curves show the distribution of X-ray absorption. The time in the horizontal axis is proportional to the distance from where the electron carriers are generated in the drift region. This is because the carriers drift to the junction with a saturated velocity of 10^7 cm s^{-1} in the drift region. The height of the dashed curve for 14.4 keV at $t = 0$, f_0, is given by $0.65 \times$ PH, where PH is the peak height of the observed time response at $t = 0$. This suggests that 65% of the total events detected in the device are absorbed in the drift region at 14.4 keV. At other energies, the amount of absorption in the multiplication region is different. This might cause the slight difference between the observed curves and the dashed curves.

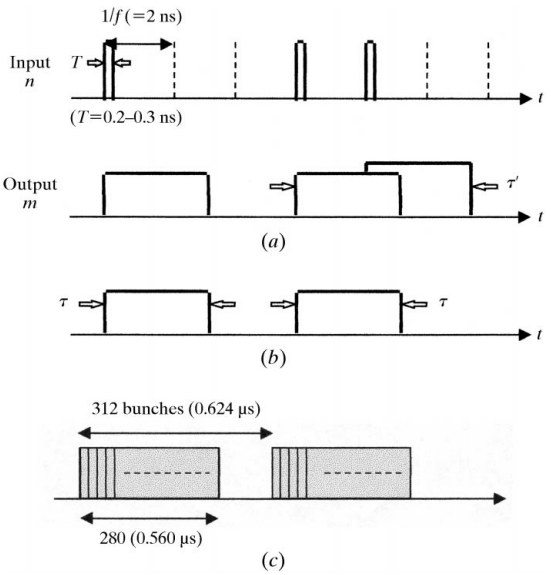

Figure 6
Behaviour of a counting system for pulsed beams. (*a*) Paralyzable, (*b*) non-paralyzable, (*c*) bunch structure for the multibunch mode of the Photon Factory ring.

The energy resolution of this device was 21% at 16.53 keV. The value was obtained with a charge-sensitive pre-amplifier (CANBERRA 2001A) and a spectroscopy system (Main Amp.: ORTEC 572, ADC: CANBERRA 8077, MCA: Fast ComTec MCD/PC). The shaping time of the main amplifier was 0.5 μs. The reverse-bias voltage for the APD was −650 V. On the other hand, another spectrum was measured using the fast-counting system. The condition for operating APDs was the same as in the measurement with the normal spectroscopy system. The pulse-height distribution was taken by scanning the threshold level of the discriminator. This method is called sequential single-channel discrimination (Knoll, 1989). Both spectra were almost the same. The pulse-height distribution at rates $>10^6$ counts s^{-1} was recorded at 8.05 keV by sequential single-channel discrimination. The distribution was not so deformed even at 18×10^6 counts s^{-1}. At higher rates of up to 10^8 counts s^{-1}, the peaks of multiple-photon events are seen. These are

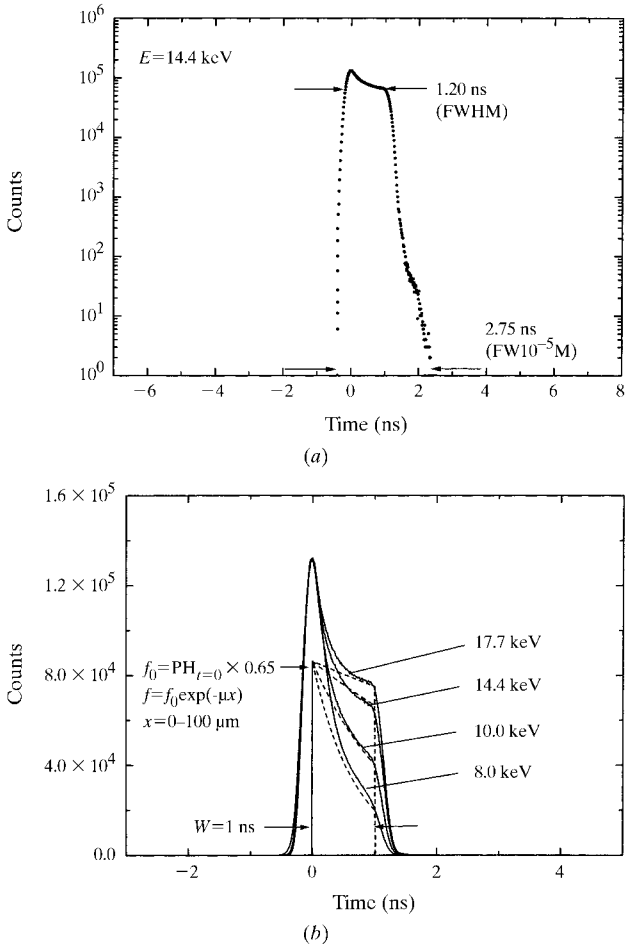

Figure 7
Time response of SPL2625: (*a*) a response function measured at 14.4 keV, and (*b*) profiles of time response measured at 8.0, 10.0 14.4 and 17.7 keV. The peak heights (PH) are normalized to the result at 14.4 keV in (*b*). The dashed curves give the distribution of X-ray absorption for each energy through the drift region (x = 0–100 μm).

caused by events where two or three photons are detected per bunch. The detector had a resolution up to 10^8 counts s^{-1}.

5. Conclusions

The APD has a sub-nanosecond time resolution. A time resolution shorter than 100 ps is possible by using a thin sensitive region <10 μm thick. The excellent resolution was applied to observe the bunch structure of a storage ring. The bunch width of 60 ps was correctly obtained for the hybrid mode of the ESRF ring with the detector using an S5343 APD device. The bunch purity was successfully measured up to 10^{-9} at the single-bunch mode of the Photon Factory ring. The fast response is useful for time spectroscopy of nuclear excitation, such as Mössbauer experiments on ^{169}Tm. This nucleus has a 4 ns half-life for the 8.4 keV excited level. The time resolution of 100 ps and a short tail in the time spectrum may help to record a clear structure in time.

The APD is able to have a high efficiency by employing a stack of devices having a transmission structure. An SPL2625 device has a sensitive region 120–130 μm thick. A detector using a stack of four SPL2625 devices was fabricated. The output rate per device reached more than 10^8 counts s^{-1} and the lower limit was less than 10^{-2} counts s^{-1}. Thus, the APD detector had a wide dynamic range of more than 10^{10}.

The pulse-height distribution was measured up to 10^8 counts s^{-1} by single-channel sequential discrimination. The SPL2625 device has an energy resolution better than that of an NaI detector at room temperature and at a gain of ~50. Moreover, at low temperature the dark current of the device decreases, and the deviation caused by multiplication decreases with smaller gain. Therefore, an APD may have a better resolution at a low temperature and at a small gain. If an APD detector has a high efficiency, high-rate capability and a good energy resolution, these properties enable us to carry out further new applications in synchrotron radiation.

References

Baron, A. Q. R. (1995). *Nucl. Instrum. Methods*, A**352**, 665–667.

Baron, A. Q. R. & Ruby, S. L. (1994). *Nucl. Instrum. Methods*, A**343**, 517–526.

Kishimoto, S. (1992). *Rev. Sci. Instrum.* **63**, 824–827.

Kishimoto, S. (1994). *Nucl. Instrum. Methods*, A**351**, 554–558.

Kishimoto, S. (1997). *Nucl. Instrum. Methods*, A**397**, 343–353.

Kishimoto, S., Ishizawa, N. & Vaalsta, T. P. (1998). *Rev. Sci. Instrum.* **69**, 384–391.

Knoll, G. F. (1989). *Radiation Detection and Measurement*, 2nd ed., pp. 652–654. New York: Wiley.

Sheidt, K. (1995). Private communication.

Squillante, M. R., Farrell, R., Lund, J. C., Sinclair, F., Entine, G. & Keller, K. R. (1986). *IEEE Trans. Nucl. Sci.* **33**, 336–339.

Toellner, T. S., Sturhahn, W., Alp, E. E., Montano, P. A. & Ramanathan, M. (1994). *Nucl. Instrum. Methods*, A**350**, 595–600.

Webb, P. P., McIntyre, R. J. & Conradi, J. (1974). *RCA Rev.* **35**, 234–278.